Research Square

Preprints are preliminary reports that have not undergone peer review.
They should not be considered conclusive, used to inform clinical practice,
or referenced by the media as validated information.

Optimising Viscoelastic Window in Reversible Liquid Crystal Elastomer-Based Pressure Sensitive Adhesives via Chain Transfer

Mohand Saed

mos29@cam.ac.uk

University of Cambridge https://orcid.org/0000-0001-7251-0227

Lichang Lu

University of Cambridge

Kailing Lin

University of Cambridge

Article

Keywords:

Posted Date: April 9th, 2026

DOI: https://doi.org/10.21203/rs.3.rs-8328471/v1

License: This work is licensed under a Creative Commons Attribution 4.0 International License.
Read Full License

Additional Declarations: There is **NO** Competing Interest.

Version of Record: A version of this preprint was published at Communications Materials on July 10th, 2026. See the published version at https://doi.org/10.1038/s43246-026-01260-4.

Abstract

Reversible adhesives that can be debonded and reused on demand are essential for next-generation sustainable electronics assembly, biomedical devices, and soft reconfigurable systems. Liquid crystal elastomer (LCE) exhibits dynamic adhesion leveraging their thermomechanical responsiveness and tunable bulk rheological behaviour. However, existing LCE adhesives often require extended contact period or thermal annealing to attain sufficient tack, which significantly limits their broader application. Here, we present a scalable chain-transfer reaction strategy using commercially available agents to directly regulate the viscoelastic properties of LCEs. This approach enables an 'ideal' pressure-sensitive adhesive (PSA), satisfying the Dahlquist criterion without any tackifier or thermal conditioning while maintaining the excellent reversibility. The resulting LCEs exhibit a low glass transition temperature (−11°C) and a storage modulus of 0.1 MPa at room temperature. They also display strong adhesion owing to their exceptional viscoelastic dissipation, with a peak loss factor (tan δ) of 1.85 and a broad high damping plateau (tan δ ≈ 0.91) within the nematic phase. Remarkably, both the peel and tack strengths remain comparable before and after annealing, outperforming conventional LCE-based adhesives that depend on time- or heat-assisted wetting. This work provides a new design strategy for high-performance, debondable, and reusable adhesives, paving the way for more sustainable and smart adhesive technologies.

Introduction

Polymer adhesives play a crucial role across diverse sectors, from industrial manufacturing to everyday consumer products[1,2]. Their large usage volume significantly impacts both economic efficiency and environmental sustainability[3]. Amongst these materials, pressure-sensitive adhesives (PSAs) represent a unique class of lightly crosslinked polymers that are permanently tacky at room temperature, enabling firm adhesion to a variety of surfaces with only light fingertip pressure[4]. This property makes them widely used in household, medical tapes, electronic devices, packaging, and automotives applications[5,6]. However, most PSAs remain difficult or impossible to be reused or recycled due to surface contamination, adhesion fatigue after detachment and their permanently covalent crosslinked molecular structures[7,8]. Current end-of-life strategies often involve energy-intensive chemical recycling processes requiring harsh solvents or environmentally unsustainable landfilling practices[9].

Reversible PSAs, designed to release adhesion on demand through environmental stimuli, provides opportunities for multi-use applications and contributes to reducing unrecyclable plastic waste[10]. Such adhesives have shown great potential in robotics, wearable devices and manufacturing assembly[11,12]. A wide range of strategies have been developed to engineer adhesives that can detach on demand, including dynamic covalent chemistries, photo-isomerisation, supramolecular interactions, or hierarchical surface designs[13–17]. While each of these approaches offers useful switching behaviours, many depend on intricate chemistry or sophisticated surface and interface architectures that limit scalability and often lead to cyclic adhesion deterioration.

Liquid crystal elastomers (LCEs) offer a fundamentally different and compelling route owing to their enhanced energy dissipation, reversible bulk viscoelasticity, and phase-dependent adhesion[18]. As a class of loosely crosslinked polymeric material, LCEs integrate rubber elasticity of polymer networks with the orientational order of liquid crystals[19–21]. Traditionally, LCEs have been regarded as versatile, multifunctional reversible actuating materials, yet recent studies by Terentjev and coworkers have uncovered their potential for reversible adhesion[22–25]. The concept of adhesion reversibility is assumed to be governed by the nematic-isotropic phase transition[26]. The observed dynamic adhesion originates from the substantial viscoelastic contrast between two phases – specifically, a high loss factor (i.e. tan δ) in nematic phase and a reduced loss factor in the isotropic phase[26]. In particular, the elevated energy dissipation observed in the nematic phase arises from the internal rearrangement of liquid crystal molecules coupled with friction and entanglement of polymer chains. This synergy produces remarkably high tan δ at room temperature, often exceeding 1, far above those of conventional viscoelastic systems[27,28]. Once the liquid-crystal ordering collapses in the isotropic phase, this dissipation mechanism largely disappears[29]. As the field continues evolving, substantial efforts have been dedicated to improving adhesion strength, investigating the mechanism, and exploring multi-signal responsiveness[30–32].

However, despite these advances, a major practical constraint still prevents LCE reversible adhesives from achieving broader real-world adoption. Nearly all reported LCE systems require extended contact time or annealing to soften the network and allow sufficient wetting before strong adhesion develops. This necessity originates from the inherently high modulus of conventional LCEs, typically ~ 10 MPa, caused by rigid mesogens that are placed in the main chain LCE networks or high crosslink density. In order for LCEs to function as ‘ideal’ PSAs without pre-treatment, LCEs must instead satisfy the Dahlquist criterion: a glass transition temperature (T_g) below 0°C and a rubbery storage modulus (E') below 0.3 MPa at 1 Hz[33]. While our group recently demonstrated that side-chain siloxane LCE adhesives can meet this requirement and deliver strong, reversible adhesion, the siloxane route relies on customised mesogen synthesis that limits accessibility and scalability[34].

Acrylate-based materials dominate the commercial PSAs market, accounting for approximately 60–70% of total production[35]. Their broad adoption arises from the cost-effective starting materials, superior adhesive performance, and ease of processability[35]. The wide range of available acrylate monomers also provides flexibility in tailoring mechanical, optical, chemical, and thermal properties. In addition, most acrylate monomers are typically low-viscosity liquid that mix easily with initiators, crosslinkers, and additives. They polymerise efficiently via free-radical mechanisms, enabling rapid curing through thermal, redox, or UV initiation. However, translating acrylate chemistry into LCE-based PSAs is challenging. Radical polymerisation of acrylate-based mesogens typically produces glassy liquid-crystalline polymer networks with high T_g (≈ 50–100°C) and high E' (≈ 10–100 MPa), far above the Dahlquist criterion for ‘ideal’ PSA performances. Meeting this criterion must require substantially lowering the crosslink density of these highly crosslinked networks. The most effective approach to reducing crosslink density in

acrylate system is the use of chain transfer agents (CTAs) such as mercaptans (i.e. thiols), Living Free-Radical Polymerisation by Reversible Addition-Fragmentation Chain Transfer (RAFT), cobalt compounds, or carbon tetrachloride agents[36–38]. Among these, thiols-based CTAs have proven particularly effective in modulating the crosslink density of acrylate-based LCEs, which has been successfully applied for actuators[39–41].

Here, we present a simple, robust, scalable chain transfer-controlled approach that enables the first reversible acrylic-based LCE adhesives to satisfy the Dahlquist criterion. Using commodity mesogens (RM257) and straightforward photopolymerisation, we incorporate 2,2-(ethylenedioxy)diethanethiol (EDDT) as a CTA to regulate network structure, reducing the crosslink density, and therefore, lowering modulus while preserving the intrinsic reversible viscoelastic behaviour of LCEs. Unlike conventional thiol-acrylate click chemistry, where thiol participates in step-growth polymerisation, here dithiols terminate the growing chain and initiate a new chain propagation. By systematically optimising the monomer-to-CTA ratio, the resulting LCEs achieve a T_g of ~ -11°C and a room-temperature storage modulus of 0.1 MPa, meeting the Dahlquist criterion while enabling immediate, annealing-free tack. Furthermore, the LCEs display an exceptional loss factor (tan δ) of ~ 1.85 at T_g and maintain a high tan δ of 0.91 in the nematic phase, consistent with strong viscoelastic adhesion. Overall, this work establishes a practical and accessible route to high-performance, reversible acrylic-based LCE adhesives, paving the way towards more sustainable and reusable PSA technologies.

Experimental

2.1. Materials

1,4-Bis-[4-(3-acryloyloxypropyloxy)benzoyloxy]-2-methylbenzene, (RM257) was purchased from Chemfish. Ltd. 2,2-(ethylenedioxy)diethanethiol (EDDT) and 2,2-Dimethoxy-2-phenylacetophenone (Irgacure 651, i651), and toluene were purchased from Sigma-Aldrich and used as received.

2.2. Preparation of liquid crystal elastomer

The liquid crystal elastomer was synthesised via a chain transfer reaction approach, as illustrated in Fig. 1a. RM257 was first dissolved in toluene (30 wt.%) at 85°C in oven. Subsequently, 1 wt.% of i651 was added to the RM257 solution. Various molar ratios of RM257 and EDDT (1:1, 1:1.5, and 1:2) were employed, with EDDT serving as the chain transfer agent. The resulting mixture underwent vigorous mixing using a Hauschild Speed Mixer (800 rpm for 10 s and 2000 rpm for 120 s) under vacuum for degassing.

2.3. Fabrication of LCE adhesive tapes

The prepared mixture was cast onto a plasma-treated polyethylene terephthalate (PET) film (23 μm, Hi-Fi Industrial Film Ltd) to ensure strong interfacial bonding and mounted on a 75°C hot plate. The PET backing film was plasma-treated using a Diener Plasma GmbH& Co. KG. The coating was performed

with a Tape casting coater (MSK-AFA-III, MTI corporation) to achieve a thickness of ca. 400 μm, followed by ultraviolet (UV) curing for 30 min. The coated films were then placed in an oven at 85°C overnight to remove residual solvent. To prevent surface contamination, the exposed LCE adhesive layer was protected with silicone release paper (backing paper from Avery labels). The final LCE adhesives tapes exhibited a homogeneous polydomain structure with a thickness of ca. 250 μm.

2.4. Preparation of free-standing LCE samples

For free-standing films, the pre-crosslinked mixture was poured into a polytetrafluoroethylene (PTFE) mould for anti-adhesion purpose and cured under UV light for 30 min, followed by solvent removal in an 85°C oven overnight.

2.5 Characterisations

Polarised optical microscopy (POM) was performed using an Olympus BX41 microscope to characterise the birefringence of the LCE. The polariser and analyser were arranged at relative angles of 0° and 45°.

The Differential scanning calorimetry (DSC) was conducted using a TA instrument DSC Q200. Approximately 10 mg of each sample was sealed in standard aluminum pans. The samples were heated from room temperature to 100°C at a rate of 5°C min^{-1}, held isothermally for 5 min to erase thermal history, then cooled to − 50°C at the same rate and held for another 5 min, followed by another heating cycle from − 50°C to 100°C at the same rate. Data from the third heating cycle was used to determine the glass transition temperature (T_g) and nematic-isotropic temperature (T_{ni}).

Fourier transform infrared (FTIR) spectroscopy was performed on pre- and post-curing samples to characterise the reaction rate using the Thermo Scientific Nicolet iS10 spectrometer, with 16 scans recorded in the range of 4000–600 cm^{-1}. The peak of unreacted aromatic ring (band near 1600 cm^{-1}, C = C stretching vibration within the benzene ring) was used as internal reference for normalisation.

The thermomechanical properties of the LCE (10 × 2 × 1 mm) were characterised by using a TA Instruments DMA850 in tension film mode. The temperature was ramped from − 100 to 150°C at a 2°C min^{-1} while the samples were oscillating at 0.02% strain at a frequency of 1 Hz. The storage modulus (E'), loss modulus (E''), and loss factor ($\tan \delta = E''/E'$) were continuously recorded throughout the temperature sweep.

Gel fraction was determined by comparing the initial mass of each LCE formulation with the remaining mass after solvent extraction. Rectangular specimens (10 × 2 × 1 mm) were immersed in toluene for 72 hours to remove soluble components. The extracted samples were then dried in an oven at 85°C overnight and reweighed to obtain the insoluble fraction.

The 180° peel adhesion tests were conducted following the ASTM D3330 standard using a Tinius Olsen ST1 tensiometer equipped with the appropriate clamping fixture. LCE adhesive tapes were tested both with and without annealing to evaluate their pressure-sensitive adhesive performance. During testing, the

tapes were peeled from the metal substrate at a constant rate of 300 mm min^{-1}. For elevated-temperature measurements, the adhesive tapes were pre-heated on a hot stage to the designated temperature prior to performing the same peeling procedure.

The probe tack testing protocol was adapted from previous studies[30]. A spherical stainless-steel probe (10 mm diameter) was mounted on a vertical dynamometer frame (Tinius Olsen). Before each test, the probe was cleaned with acetone and brought into contact with the LCE adhesive layer, which was affixed to a flat rigid substrate and secured with a bottom clamp. Upon reaching a contact load of − 0.5 N, the probe was held in contact and allowed 300 s dwell time to ensure interfacial equilibration. It was then withdrawn at a constant rate of 10 mm min^{-1} while continuously recording the force.

Results and Discussion

The main goal of this study is to remove the need for extended contact time or annealing while maintaining the reversible adhesion and maximising viscoelastic dissipation. Two key factors are therefore considered, namely low room-temperature storage modulus and low glass transition temperature. These parameters enable the LCE-based reversible adhesives to satisfy the Dahlquist criteria, functioning as 'ideal' PSAs. In contrast to thiol-acrylate click chemistry[42], where thiols were employed to initiate step-growth, here EDDT acts as a chain transfer agent during the radical homopolymerisation of acrylate mesogens. The propagating acrylate radicals abstract hydrogen atoms from EDDT, generating thiyl radicals while terminating the growing chain. These thiyl radicals subsequently reinitiate polymerisation, producing new chain segments (**Figure S1**). As a result, the incorporation of EDDT leads to shorter network strands, dangling chain ends, and a reduced effective crosslink density, as schematically illustrated in Fig. 1a.

Two characteristic transition temperatures of LCE systems, namely T_g and T_{ni} of various formulations, determined by DSC, are presented in Fig. 1b. Both T_g and T_{ni} decrease with increasing EDDT content. Because the higher CTA proportion dilutes mesgenic packing, less thermal energy is required to disrupt the molecular ordering[43]. The wide temperature window between T_g and T_{ni} provides good flexibility and adhesion performance for room-temperature applications. Due to the polydomain nature of the synthesised LCEs, they appear opaque in the nematic phase (below T_{ni}) owing to light scattering from randomly oriented domains and refractive index anisotropy. Upon heating above T_{ni}, the liquid crystal molecules lose long-range orientational order and transition to the isotropic phase, yielding an optically transparent film, as shown in Fig. 1c (retrieved from *Movie S1*). Their birefringence behaviour is further confirmed by POM. An aligned, free-standing monodomain LCE adhesive appears dark when the director is parallel to the analyser and bright when rotated to 45°, as shown in Fig. 1d. The LCE adhesives also exhibit distinct phase-dependent adhesion, as demonstrated in Fig. 1e (retrieved from *Movie S2*). In the nematic phase, the tackiness is sufficient to support a 500 g weight, whereas in the isotropic phase, adhesion is lost without any external stress.

Given the nature of the chain transfer reaction, two competing radical pathways coexist during polymerisation[39,41]: (i) acrylic homopolymerisation, where propagating radicals extend the polymer chain via C = C addition, and (ii) chain transfer to dithiol, where radicals abstract hydrogen from thiol groups, terminating the current chain growth and generating a new thiyl radical. Understanding the kinetic competition between them is crucial, as the resulting network architecture can strongly impact the viscoelastic properties of the LCEs. Hence the FTIR is conducted on the pre- and post-polymerised LCEs with varying mesogen to CTA ratios. Two characteristic peaks are monitored, namely vinyl = CH_2 bending (~ 810 cm^{-1}) corresponding to acrylate mesogens, and the thiol -SH stretching (2550–2600 cm^{-1}) corresponding the CTA. The spectra are normalised against aromatic C = C stretching peak at 1600 cm^{-1}, which serves as an internal reference. As shown in Fig. 2a-c, the disappearance of the 810 cm^{-1} peak confirms the complete consumption of acrylate double bonds, whereas the persistence of the S-H band indicates partial thiol conversion (~ 50%), independent of the feed ratio.

The limited thiol conversion, with no apparent dependence on the acrylic-thiol stoichiometry (Fig. 2d) is in consistency with previous study[41]. It is suspected to be associated with the different reaction environments and monomer mobility. In this system, two competing reaction mechanisms are at play: acrylate photopolymerisation and thiol-acrylate chain transfer. The acrylate polymerisation typically proceeds at a faster rate compared to the chain-transfer process. In addition, at lower EDDT content (e.g. 1:1 ratio), the system exhibits higher viscosity due to the dense packing of mesogenic monomers and the nematic-phase ordering. Both contribute to restricting diffusion and reducing the probability of chain transfer. However, increasing the concentration of thiol groups (e.g. 1:2 ratio) in the formulation with the thiol functions partly as a flowable medium, enhances mobility and promotes more chain-transfer events.

The intrinsic dynamic properties (i.e. viscoelasticity) play a crucial role in governing adhesive performances. Three key indicators, such as T_g, storage modulus, the magnitude and the range of tan δ must be considered when designing adhesives. In particular, T_g dictates whether an adhesive behaves as structural adhesives or a PSAs, storage modulus governs the ability to deform and wet a surface, and tan δ controls viscoelastic energy dissipation and adhesion strength. The dynamic viscoelastic profiles of the LCEs are characterised by DMA. Before discussing the results, the Dahlquist criterion is reiterated here that 'ideal' PSAs require a T_g below 0°C and a room-temperature storage modulus (E') below 0.3 MPa at 1Hz.

In the glassy state (-100°C), all formulations exhibit similar storage modulus irrespective of the RM257:EDDT ratio because the temperature is well below T_g, and the stiffness is dominated by local bond vibrations rather than network structure. Once the temperature exceeds T_g and the material enters the rubbery phase, the influence of EDDT becomes pronounced. Higher EDDT content increases the possibility of chain-transfer events, thereby reducing the effective crosslink density and lowering the E'. The resulting network contains fewer chain constraints and a greater number of dangling ends, which

collectively contribute to a decreased T_g (Fig. 3a). The effective crosslink density is determined following the below equations[44,45]:

$$d = \frac{G\prime}{RT}\,; G' = \frac{E\prime}{2(1+\upsilon)}$$

where d (mol cm^{-3}) denotes the crosslink density per unit volume, $G\prime$ and $E\prime$ (Pa) represent the shear modulus and rubbery modulus respectively, R (J K^{-1} mol^{-1}) is the gas constant and T (K) is the absolute temperature. υ is the Poisson ratio and approximated as 0.5 because of the rubbery nature of the LCE. Therefore, the equation can be simplified to:

$$d = \frac{E\prime}{3RT}$$

To minimise the influence of the nematic-isotropic transition on rubbery modulus, E' at 100°C is used, which is well above both T_g and T_{ni}. As detailed in **Table S1**, the crosslink density of 1:2 formulation (2.47×10^{-6} mol cm^{-3}) is two orders of magnitudes lower than 1:1 formulation (1.81×10^{-4} mol cm^{-3}), indicating the effectiveness of chain transfer approach in diluting the network junctions, as illustrated in Fig. 3b. The reduced crosslink density leads to a larger soluble fraction of the LCEs, consistent with the gel fraction results shown in **Figure S2**.

The looser network not only lowers *E'* but also enhances segmental mobility and viscoelastic dissipation, resulting in an increased tan δ. All formulations exhibit pronounced tan δ peak at T_g, reaching approximately 1.14, 1.44 and 1.85 for RM257:EDDT ratios of 1:1, 1:1.5 and 1:2, respectively. Remarkably, the LCE displays a distinct tan δ plateau above T_g. This behaviour arises from the reorientation of liquid crystal molecular at nematic phase, coupled with entanglement between the polymer chains. This unique thermomechanical feature highlights the potential of LCE for vibration damping and reversible adhesion applications for wide temperature and frequency ranges[46,47]. Upon further temperature rise, the LCEs transition from nematic to isotropic phase, leading to a drop in tan δ as mesogen-mediated dissipation vanishes. It is also notable that T_{ni} decreases with increasing EDDT content, with the 1:1 formulation exhibiting the highest and the 1:2 the lowest transition temperature. This trend arises because denser mesogenic packing in low-EDDT systems strengthens intermolecular interactions, requiring more thermal energy to disrupt the ordered configuration.

Figure 3c presents the conclusive comparison, showing that both the 1:1.5 and 1:2 formulations exhibit T_g values below 0°C. The 1:2 formulation achieves a room-temperature storage modulus below 0.3 MPa, fully satisfying the Dahlquist criterion for 'ideal' PSAs, while the 1:1.5 formulation approaches this threshold with an E' close to 0.3 MPa. Compared with the stiffer 1:1 ratio, their lower modulus enhances mesogen mobility and interfacial wetting, showing potential in eliminating the need for extended contact time or annealing to align mesogens with surface geometry for maximising the adhesion strength. All the characteristic temperatures of various formulations are concluded in **Table S2** in detail. It is worth

mentioning that the T_g detected by DMA is generally higher than that measured by DSC, which originates from the difference in the physical phenomena probed by these techniques. DSC detects when heat capacity increases due to molecular motion, while DMA detects when those motions are sufficient to affect mechanical stiffness. Because mechanical relaxation requires more mobility than thermal relaxation, T_g from DMA is usually higher.

Adhesives performances are commonly assessed through tack, peel, and shear tests, where the tack test measures the initial tackiness, the peel test reflects the energy dissipated during interfacial debonding, and the shear test evaluates the resistance to sustained shear forces. As shear tests are typically employed for structural adhesives, this study focuses on peel and tack performances. Figure 4a demonstrates the probe tack test, which can effectively quantify the initial tackiness under light pressure. In this test, a spherical metal probe is brought in contact with the adhesive surface at a target load, held under a constant dwell time of 300 s, and then retracted. As shown in Fig. 4b-c, the 1:1 formulation exhibits the lowest tack strength. This is attributed to the high crosslink density and correspondingly high rubbery modulus, leaving few mobile or dangling chains available for interfacial bonding. Increasing the content of EDDT reduces the effective crosslink density and introduces more chain mobility, leading to a higher tackiness. In particular, the 1:2 formulation displays a distinct force plateau following the initial peak, characteristic of fibrillation during debonding. This process involves the formation and elongation of adhesives, which dissipate additional energy and thereby enhance the adhesion strength.

A 180° peeling test is conducted following the industrial standard ASTM D3330 (Fig. 4d). Figure 4e-f presents the peel force-displacement curves for LCEs formulations, tested both with and without annealing. The as-prepared 1:1 formulation expectedly exhibits a lower peel strength, attributed to its high storage modulus that limits interfacial wetting thereby reducing the bonding strength between LCE and the substrate. Annealing significantly increases adhesion by three times through reducing the modulus and enhancing chain mobility at the interface, which improves substrate wetting. In contrast, the 1:1.5 and 1:2 formulation exhibit comparable peel forces before and after annealing. The slight improvement observed after annealing arises from the thermally accelerated mesogenic alignment along the substrate surface geometry, an effect that can alternatively be achieved by extending the contact time, as reported in previous studies[30,32]. Notably, oscillatory stick-slip patterns are observed, particularly in the 1:1.5 and 1:2 formulation. This is likely caused by the delayed response of mesogenic reorientation during peeling at a quick rate like 300 mm min^{-1}. Reducing the peeling rate allows more time for molecular relaxation, thereby mitigating the stick-slip effect (**Figure S3**).

A summary plot of the normalised peel forces across different formulations is presented in Fig. 4g. A considerable increase from the as-prepared to the annealed state is observed for the 1:1 sample, consistent with its modulus reduction and improved wetting upon annealing. In contrast, the 1:1.5 and 1:2 formulations show comparable peel forces with and without annealing. Furthermore, the tack force follows a clear trend: with increasing EDDT content, the LCE adhesives become progressively tackier and more energy dissipative. The nearly identical tack forces for the annealed and as-prepared samples

confirm the practical reliability of the developed LCE adhesives. Compared with commercial PSAs, LCE adhesives generally exhibit stronger peeling strength as shown in Fig. 4h, driven by the additional energy dissipation arising from the mesogenic reorientation during deformation. The exception is the 1:1 formulation, whose comparatively high room-temperature modulus limits effective wetting and therefore suppresses adhesion. Notably, the chain-transfer LCE (CT-LCE) samples display annealing-independent peel performances, in clear contrast to previously reported thiol-acrylate LCE system.

A defining characteristic of LCE-based adhesives is their stimuli-responsive detachment capability, where they maintain strong adhesion under service conditions while allowing clean release upon activation. As shown in Fig. 5a (retrieved from *Movie S3-4*), below the T_{ni} (i.e. within the nematic phase), the LCE adhesive tapes adhere firmly to the glass substrate and are capable of holding a 500 g weight, indicating its strong bonding. When the temperature rises above T_{ni} and the LCE transitions into the isotropic phase, the adhesion diminishes, facilitating effortless peeling. Furthermore, this reversible adhesion exhibits good cycling stability over at least five heating-cooling cycles, as demonstrated in *Movie S5*.

To quantitatively evaluate the thermal responsiveness of the LCE adhesives, 180° peel and probe tack tests are performed at elevated temperatures. As shown in Fig. 5b, the peel force decreases sharply upon heating, dropping significantly at 50°C when the adhesives transitions into the isotropic phase. Further temperature increases result in an almost complete loss of peel strength, corresponding to their suppressed viscoelastic energy dissipation (i.e. reduced tan δ) at high temperatures. In all cases, the substrate surfaces remain residue-free after detachment (**Figure S4***a-b*), confirming that debonding proceeds through interfacial failure rather than cohesive rupture (**Figure S4***c*). This indicates that the LCE adhesives maintain their structural integrity during service and enable clean, thermally induced debonding on demand. The temperature-dependent tack behaviour is presented in Fig. 5c. Compared with the sharp decline in peel strength, tackiness decreases more gradually with temperature, with approximately 50% of its maximum value retaining at 70°C. This contrast reflects the different deformation modes probed by the two tests: peeling primarily depends on dynamic viscoelastic dissipation, which is highly temperature-sensitive, whereas tack reflects the quasi-static interfacial compliance of the adhesive, which diminishes more gradually with temperature.

This thermally induced debonding is particularly promising for next-generation technologies, such as biomedical wearables and reconfigurable assemblies. In Fig. 5d-e (retrieved from *Movie S6-7*), the LCE adhesives exhibit strong adhesion on rubber gloves, functioning as potential biomedical adhesive interfaces for attaching physical sensors. Upon mild heating, the transition from nematic to the isotropic phase enables pain-free and residue-free removal, offering clear advantages for patient comfort and device reusability. Furthermore, the LCE adhesives are employed to bond the 3D-printed parts (Fig. 5f-g, retrieved from *Movie S8-9*), where clean thermal debonding is again observed between parts. Collectively, these demonstrations on metal, plastic, rubber, and glass substrates highlight the universality and practicality of LCE-based pressure sensitive adhesives for diverse applications requiring on-demand debonding and reversible adhesion.

Conclusion

In conclusion, this work establishes a transformative pathway for designing debondable pressure-sensitive adhesives based on liquid crystal elastomers. The proposed chain-transfer reaction strategy regulates the polymer networks, unlocking the optimal viscoelastic window of LCEs. The low glass-transition temperature (− 11°C) and room-temperature storage modulus of 0.1 MPa are achieved, satisfying the Dahlquist criteria without plasticisers, tackifiers, or post-annealing. The resulting LCEs exhibit remarkable energy dissipation (tan δ ≈ 1.85 at T_g; tan δ ≈ 0.91 in nematic phase) and strong yet reversible adhesion (peel ≈ 1.08 N mm^{-1}; tack ≈ 2.3 N) that remain stable over multiple adhesion-debonding cycles. Upon heating through the nematic-isotropic transition, the peel strength drops sharply to ~ 0.004 N mm^{-1}, enabling clean, on-demand thermal debonding. The chain-transfer approach eliminates the need for time- or heat-assisted wetting, greatly enhancing practicality of LCE-based adhesives. It further offers a scalable and additive-free platform for debondable adhesives with universal applicability across metals, plastics, rubbers and glass. This breakthrough paves the way for next generation sustainable manufacturing assemblies, biomedical wearables, and reconfigurable soft systems.

References

1. Raos G, Zappone B (2021) Polymer Adhesion: Seeking New Solutions for an Old Problem#. Macromolecules 54:10617–10644
2. Heinzmann C, Weder C, De Espinosa LM (2016) Supramolecular polymer adhesives: advanced materials inspired by nature. Chem Soc Rev 45:342–358
3. Westerman CR, McGill BC, Wilker JJ (2023) Sustainably sourced components to generate high-strength adhesives. Nature 621:306–311
4. Wang G, Huang X, Zhou Z, Zhang Y, Yu Y (2024) Enabling (De)bonding on-demand with optically switchable pressure sensitive adhesive tape via photodimerization. Chem Eng J 499:155820
5. Creton C (2003) Pressure-sensitive adhesives: An introductory course. MRS Bull 28:434–439
6. Soft Ternary -Semirings, Ravi Kumar -I (2016) Fracture and adhesion of soft materials: a review. Rep Prog Phys 79:046601
7. Klungness JH, Doshi MR (1992) Adhesive Contaminants (Stickies) and Methods for Removal. *MRS Proceedings* 266, 257–267
8. Recycling Pressure-Sensitive Products | 2012-03-19 | Adhesives Magazine | Adhesives & Sealants Industry. https://www.adhesivesmag.com/articles/90893-recycling-pressure-sensitive-products
9. Albanese KR et al (2023) Building Tunable Degradation into High-Performance Poly(acrylate) Pressure-Sensitive Adhesives. ACS Macro Lett 12:787–793
10. Packham DE (2009) Adhesive technology and sustainability. Int J Adhes Adhes 29:248–252
11. Chu B, Jung K, Han CS, Hong D (2010) A survey of climbing robots: Locomotion and adhesion. Int J Precis Eng Manuf 11:633–647

12. Kim S et al (2010) Microstructured elastomeric surfaces with reversible adhesion and examples of their use in deterministic assembly by transfer printing. *Proceedings of the National Academy of Sciences* 107, 17095–17100
13. Lee H, Lee BP, Messersmith PB (2007) A reversible wet/dry adhesive inspired by mussels and geckos. Nature 448:338–341
14. Liu Z, Tang Y, Chen Y, Lu Z, Rui Z (2024) Dynamic covalent adhesives and their applications: Current progress and future perspectives. Chem Eng J 497:154710
15. Mulcahy KR, Kilpatrick AFR, Harper GDJ, Walton A, Abbott AP (2022) Debondable adhesives and their use in recycling. Green Chem 24:36–61
16. Feldstein MM et al (2014) Thermo-switchable pressure-sensitive adhesives based on poly(N -vinyl caprolactam) non-covalently cross-linked by poly(ethylene glycol). Macromolecules 47:5759–5767
17. Kamperman M, Synytska A (2012) Switchable adhesion by chemical functionality and topography. J Mater Chem 22:19390–19401
18. Farre-Kaga HJ et al (2022) Dynamic Pressure Sensitive Adhesion in Nematic Phase of Liquid Crystal Elastomers. Adv Funct Mater 32:2110190
19. Warner M, Terentjev EM (2007) Liquid Crystal Elastomers. Oxford Univ. Press
20. Saed MO, Gablier A, Terentjev EM (2021) Exchangeable Liquid Crystalline Elastomers and Their Applications. Chem Rev 122:4927–4945
21. Terentjev EM (2025) Liquid Crystal Elastomers: 30 Years After. Macromolecules 58:2792–2806
22. Chen G et al (2023) Programming actuation onset of a liquid crystalline elastomer via isomerization of network topology. Nat Commun 14:1–9
23. Guin T et al (2018) Layered liquid crystal elastomer actuators. Nat Commun 9:1–7
24. Yao Y et al (2023) Enabling liquid crystal elastomers with tunable actuation temperature. Nat Commun 14:1–11
25. Saed MO et al (2019) Molecularly-Engineered, 4D-Printed Liquid Crystal Elastomer Actuators. Adv Funct Mater 29:1806412
26. Ohzono T et al (2019) Enhanced Dynamic Adhesion in Nematic Liquid Crystal Elastomers. Adv Mater 31:1902642
27. Efstathiou S, Nurumbetov G, Ross A, Li Y, Haddleton DM (2024) Moisture-cured solvent free silylated poly(ether-urea) pressure-sensitive adhesives (PSAs) for use as skin adhesives for application in transdermal drug delivery (TDD). Mater Adv 5:3396–3410
28. Xue W et al (2025) Biobased Itaconate Acrylic Pressure-Sensitive Adhesives via Emulsion Polymerization: Sustainable Design for High Peel Resistance. ACS Omega 10:42494–42506
29. Warner M, Bladon P, Terentjev EM (1994) Soft elasticity — deformation without resistance in liquid crystal elastomers. J Phys II 4:93–102
30. Gou H, Hou S, Saed MO, Strong (2024) Reversible, Heat-Activated Adhesion from Liquid Crystal Polymer Networks. Adv Mater Interfaces 11:2400488

31. Ohzono T, Norikane Y, Saed MO, Terentjev EM (2020) Light-Driven Dynamic Adhesion on Photosensitized Nematic Liquid Crystalline Elastomers. ACS Appl Mater Interfaces 12:31992–31997
32. Guo H, Saed MO, Terentjev EM (2023) Mechanism of Pressure-Sensitive Adhesion in Nematic Elastomers. Macromolecules 56:6247–6255
33. Abbott S (2020) Sticking Together: The Science of Adhesion. RSC Publishing
34. Koshimizu N, Saed MO (2025) Switchable pressure-sensitive adhesion in nematic side-chain liquid-crystal elastomers. Macromolecules 58:12191–12200
35. Robert Czech Z (2024) Pressure-sensitive acrylic adhesives (PSAs): how it began and the present state of art. *ChemTexts 2024 10:3* 10, 6-
36. Gridnev AA, Ittel SD (2001) Catalytic Chain Transfer in Free-Radical Polymerizations. Chem Rev 101:3611–3659
37. Chiefari J et al (1998) Living Free-Radical Polymerization by Reversible Addition – Fragmentation Chain Transfer: The RAFT Process. Macromolecules 31:5559–5562
38. Matyjaszewski K, Davis TP (2003) Handbook of radical polymerization. Handb Radical Polymerization 1–923
39. Godman NP, Kowalski BA, Auguste AD, Koerner H, White TJ (2017) Synthesis of Elastomeric Liquid Crystalline Polymer Networks via Chain Transfer. ACS Macro Lett 6:1290–1295
40. Hebner TS, Korner K, Bowman CN, Bhattacharya K, White TJ (2023) Leaping liquid crystal elastomers. Sci Adv 9
41. Hebner TS et al (2021) Polymer Network Structure, Properties, and Formation of Liquid Crystalline Elastomers Prepared via Thiol–Acrylate Chain Transfer Reactions. Macromolecules 54:11074–11082
42. Yakacki CM et al (2015) Tailorable and programmable liquid-crystalline elastomers using a two-stage thiol–acrylate reaction. RSC Adv 5:18997–19001
43. Saed MO et al (2017) High strain actuation liquid crystal elastomers via modulation of mesophase structure. Soft Matter 13:7537–7547
44. Zheng N, Fang G, Cao Z, Zhao Q, Xie T (2015) High strain epoxy shape memory polymer. Polym Chem 6:3046–3053
45. Ding Z, Yuan L, Liang G, Gu A (2019) Thermally resistant thermadapt shape memory crosslinked polymers based on silyl ether dynamic covalent linkages for self-folding and self-deployable smart 3D structures. J Mater Chem Mater 7:9736–9747
46. Choi S et al (2025) Harnessing Extreme Internal Damping in Polyrotaxane-Incorporated Liquid Crystal Elastomers for Pressure-Sensitive Adhesives. Adv Funct Mater 35:2413824
47. Saed MO et al (2021) Impact damping and vibration attenuation in nematic liquid crystal elastomers. *Nature Communications 2021 12:1* 12, 1–7

Figures

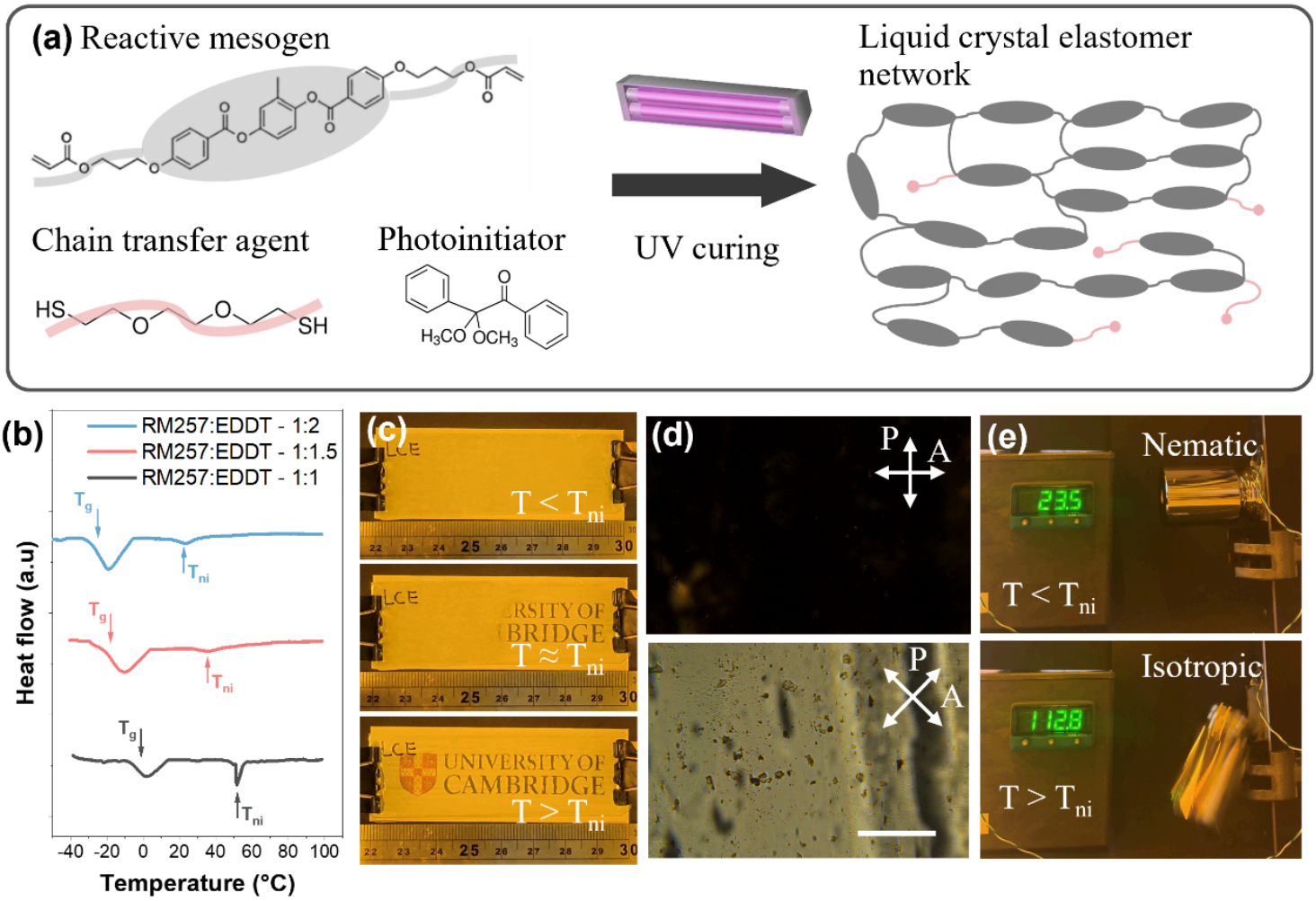


Figure 1

(a) Schematic illustration of the chain-transfer reaction mechanism and the resulting network of LCEs, (b) Differential scanning calorimetry thermograms of the LCEs with various formulations. (c) Optical appearance of RM257:EDDT - 1:1.5 adhesive tape showing a change from opaque at nematic phase to transparent at isotropic phase as the temperature increases from below to above the nematic-isotropic transition temperature. (d) Polarised optical microscopy images of the stretched RM257:EDDT – 1:2 observed at 0° and 45° between the polariser and the analyser, with a scale bar of 100 μm. (e) Thermally induced debonding of RM257:EDDT – 1:1.5 from the nematic to the isotropic phase.

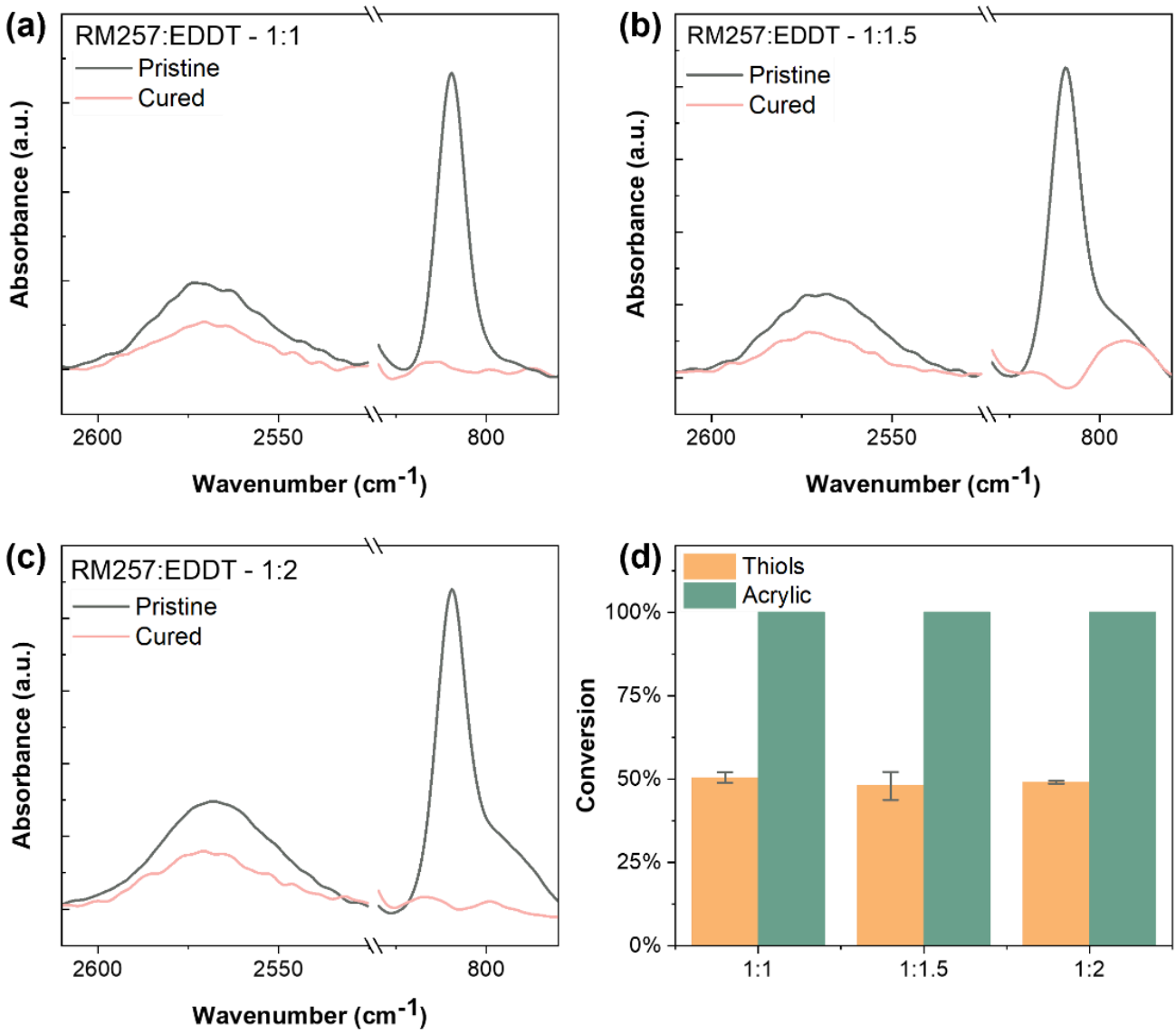


Figure 2

FTIR spectra of pre- and post-cured LCEs with different monomer-chain transfer agent ratios: (a) 1:1, (b) 1:1.5, and (c) 1:2, (d) Conversion rates of thiols and acrylate groups after UV curing for the various formulations.

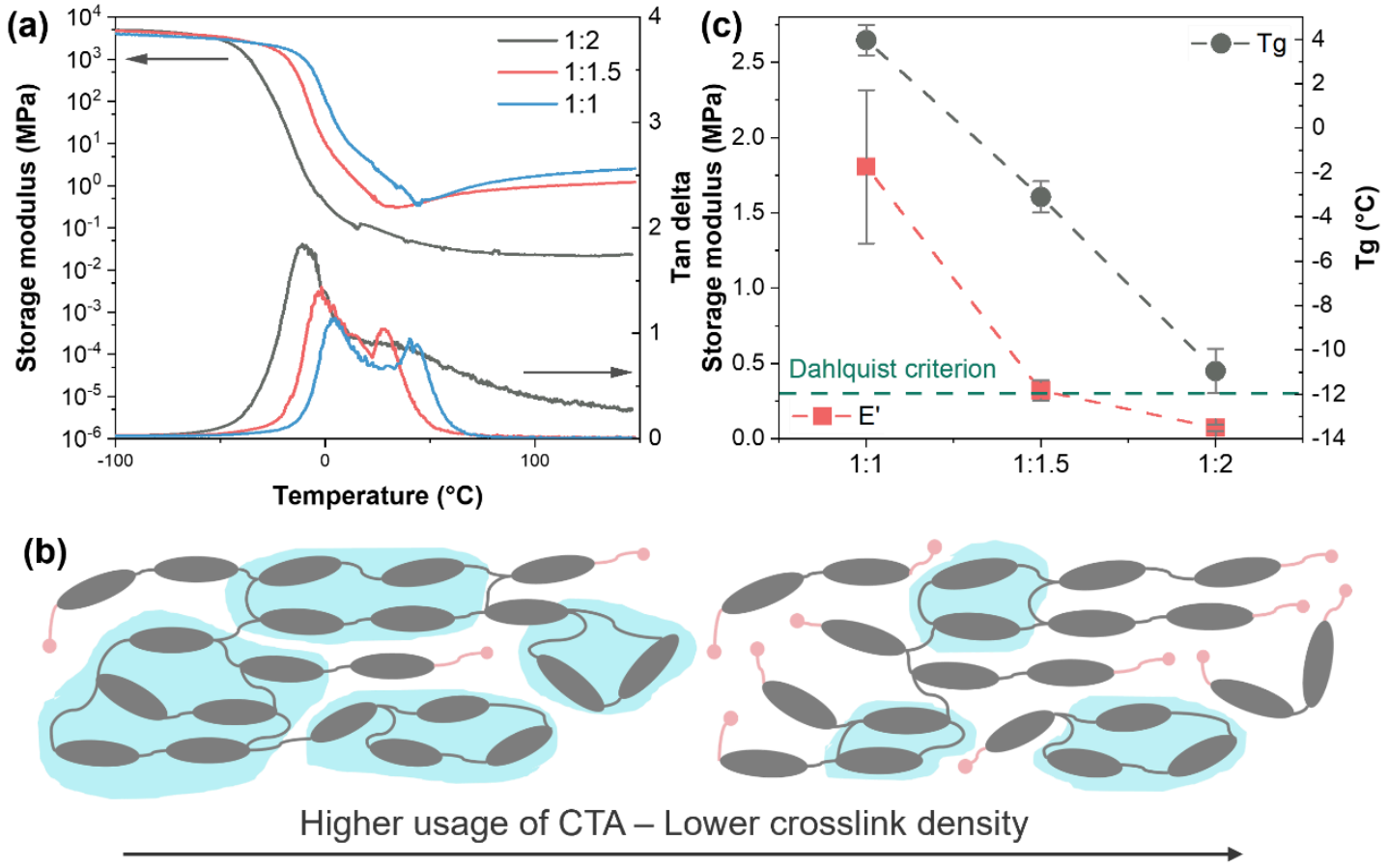


Figure 3

(a) Dynamic mechanical analysis of LCEs at various formulations with temperature scanned from -100 °C to 150 °C. (b) Schematic illustration of the effect of chain transfer agents on reducing crosslinking density and adding dangling ends, with light blue shades representing the crosslinking regions. (c) Comparison of room-temperature storage modulus and glass transition temperature of RM257:EDDT-1:1,

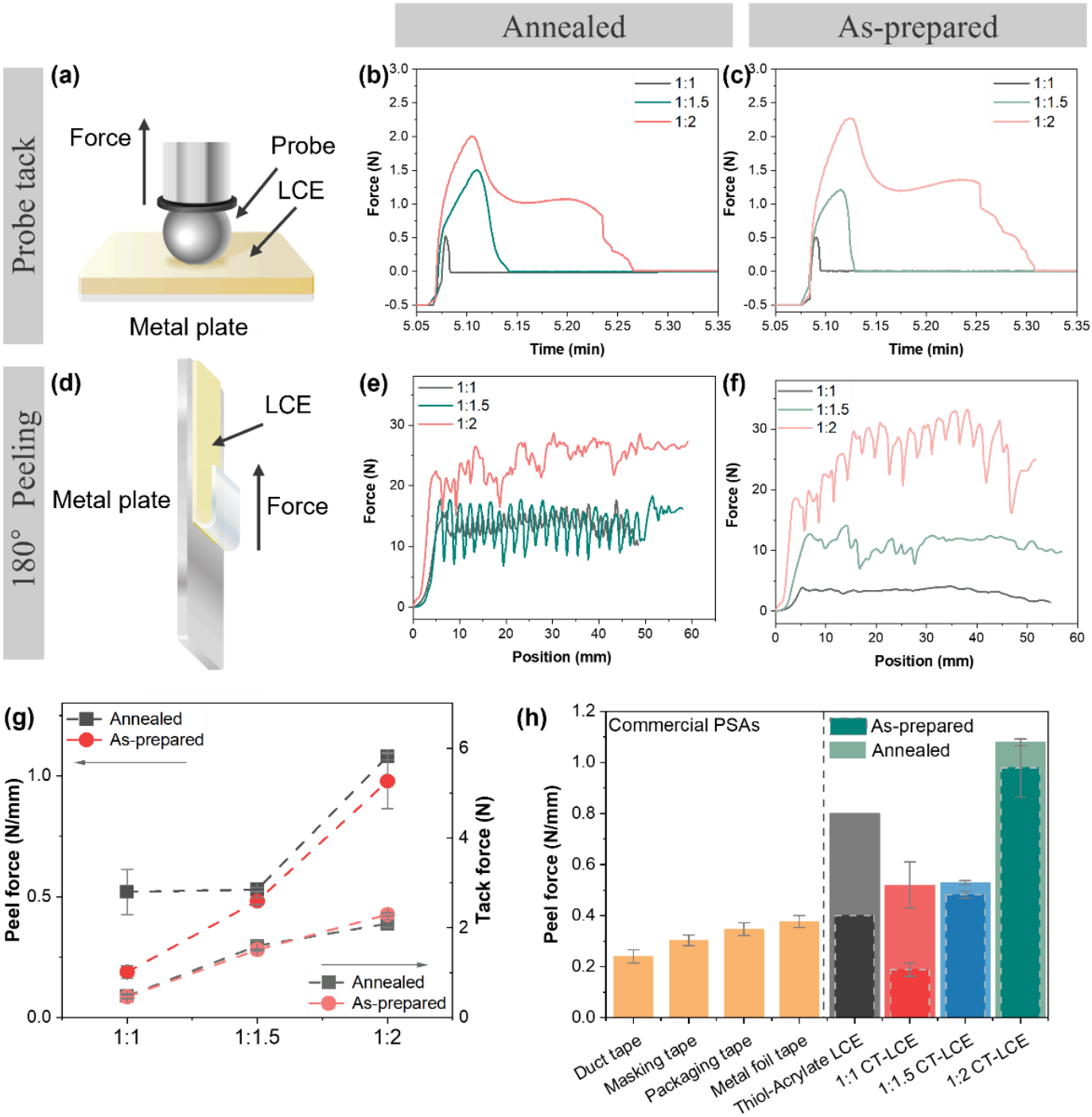


Figure 4

(a) Demonstrative diagram of the testing rig of probe tack, (b) & (c) Force – Time curves of the probe tack performance of annealed and as-prepared samples, respectively, (d) Demonstrative diagram of the testing tig of 180° peeling, (e) & (f) Force – Displacement curves of peeling performance of annealed and as-prepared samples, respectively, (g) Conclusive diagram of normalised peel force and tack force, (h) Comparison of the normalised peel force between the commercial PSAs, LCEs made by thiol-acrylate click chemistry[32] (labelled as Thiol-acrylate LCE), and made by chain transfer reaction (labelled as CT-LCE) with their as-prepared and annealed performances.

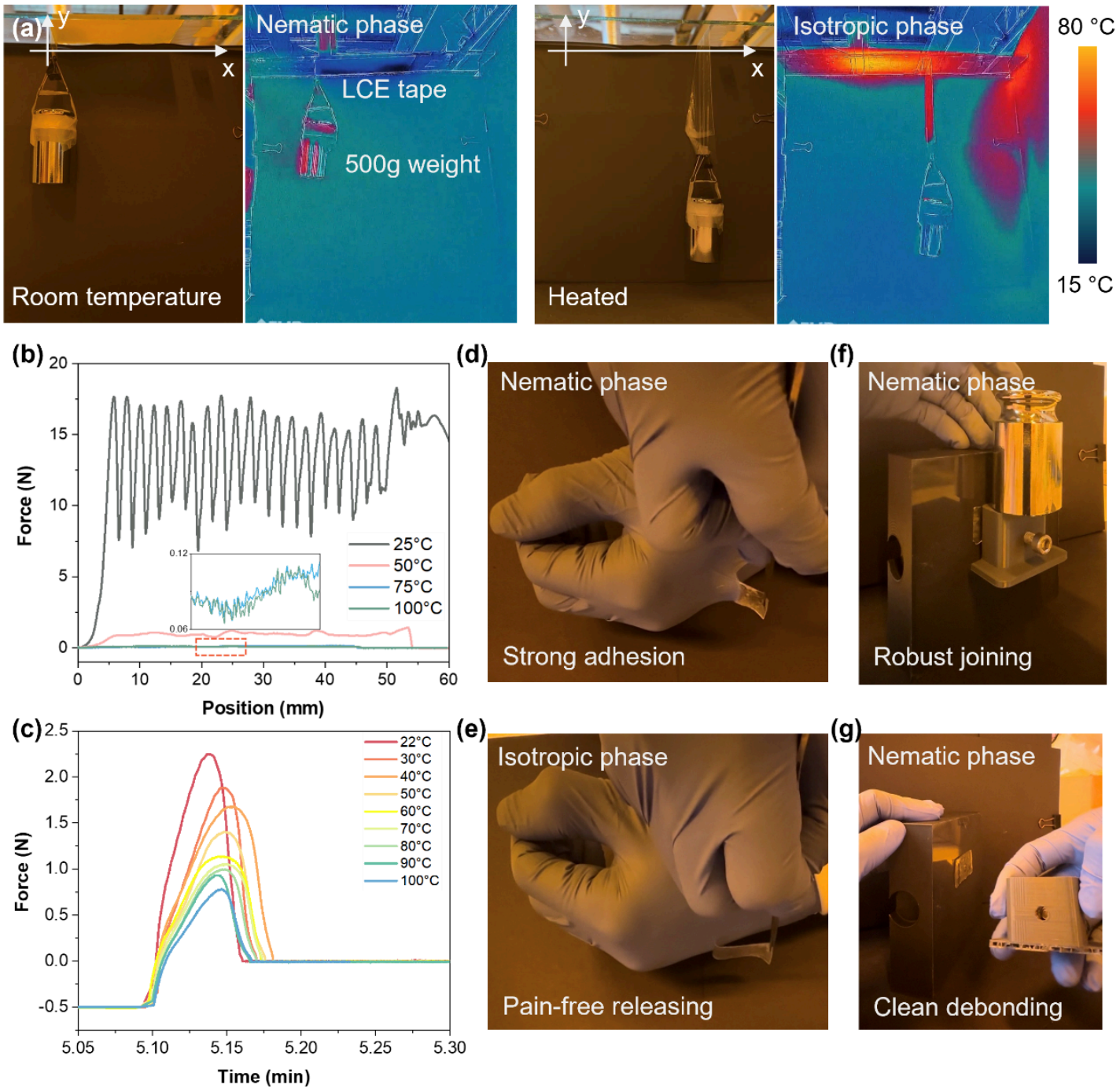


Figure 5

(a) Accelerated peeling of RM257:EDDT – 1:2 on glass substrate at elevated temperatures, (b) Peeling performances of RM257:EDDT – 1:1.5 at elevated temperatures. (c) Probe tack performances of RM257:EDDT – 1:1.5 at elevated temperatures. (d) Strong adhesion LCE-based PSA in nematic phase. (e) Pain-free releasing in isotropic phase. (f) Robust joining of 3D printed parts in nematic phase. (g) Clean debonding of 3D printed parts in isotropic phase.

Supplementary Files

This is a list of supplementary files associated with this preprint. Click to download.

- MovieS1NeatictoIsotropicdemo.mp4
- MovieS2ThermaldebondingdemoDigitalcamera2.mp4
- MovieS3ThermaldebondingdemoThermalcamera.mp4
- MovieS4ThermaldebondingdemoDigitalcamera1.mp4
- MovieS5Thermaldebonding5cycles.mp4
- MovieS6Painfreebondingdemo.mp4
- MovieS7Painfreereleasingdemo.mp4
- MovieS83Dprintedcomponentsbondingdemo.mp4
- MovieS93Dpirintedcomponentsreleasingdemo.mp4
- Supportinformation.docx